Bundle-sheath cells are leaf "water valves" controlled via xylem acidification by H^+-ATPase

One-sentence summary:

Cells enwrapping the leaf veins control the leaf hydraulic conductance by xylem sap pH regulated by a proton-pump

Noa Wigoda*[1], Yael Grunwald*[1], Nir Sade[1,2], Adi Yaaran[1], Sanbon Chaka Gosa[1], Tanmayee Torne[1], Nava Moran[1] and Menachem Moshelion[1].

[1.] The R.H. Smith Institute of Plant Sciences and Genetics in Agriculture, The R.H. Smith Faculty of Agriculture, Food and Environment, The Hebrew University of Jerusalem, Rehovot, 76100 Israel

[2.] Department of Plant Sciences, University of California Davis, Davis, CA 95616, USA

* Both authors contributed equally.

Abstract

Bundle-sheath cells (BSCs), parenchymatous cells tightly enwrapping the leaf veins, constitute selective and dynamic barrier to solutes and water. The over-three-fold-higher abundance of the AHA2 (Arabidopsis H^+-ATPase 2) transcript we reported recently in the Arabidopsis BSCs (compared to mesophyll cells) suggested AHA2 participation in this barrier function. Manipulating AHA2 activity in BSCs pharmacologically and genetically while monitoring the xylem sap pH by fluorescence imaging of FITC-dextran fed into veins of detached leaves demonstrated AHA2 necessity for low sap pH. AHA2 activity or sap acidification by buffers enhanced the hydraulic leaf conductance, while alkaline sap pH – buffered or in AHA2 knockouts – reduced it. These results resolve the decades-lasting enigma about the molecular origin of xylem sap acidification and demonstrate AHA2 importance for controlling leaf water influx.

Introduction

The majority (95%) of nutrients and water which enter the plant through the roots move upward as bulk via xylem vessels (Taiz and Zeiger, 2014) all the way into the leaf veins. On its way out of the leaf xylem and into the leaf photosynthetic tissue, the mesophyll, this transpiration stream crosses a layer of parenchymatous cells (bundle sheath cells, BSCs) which tightly enwrap the entire vasculature (Kinsman and Pyke, 1998). BSCs have been shown to act as a selective barrier between the vein and the mesophyll, capable of impeding, for example, the transport of sodium (in the banana leaf; *3*) and of boron (in the leaves of Thelungiella, *4* ; of Arabidopsis; *5*, and of banana *6*), as well as the passage of water (Shatil-Cohen et al., 2011; Pantin et al., 2013). However, it is still not clear whether and how the apoplastic (xylem) milieu modulates the "barrier behavior" of the bundle sheath, and in particular, whether this behavior depends on the xylem sap pH.

While under normal growth conditions the leaf apoplast pH is around 5.5-6 (reviewed by *9*), the much more scarce direct determinations of leaf xylem pH placed it at 6.3-6.7 in cotton leaves (Hartung et al., 1988), or at 5.3 in sunflower leaves (Jia and Davies, 2007). The leaf xylem sap pH can change in response to external conditions. For example, the leaf xylem sap alkalinized when tomato roots were exposed to drying soil or supplied with nitrate (Jia and Davies, 2007), or when detached sunflower leaves were supplied with HCO_3^- (Mengel, 1994). In turn, changes in the leaf xylem sap pH regulate physiological processes. For example, feeding high-pH solutions to detached leaves reduced stomatal conductance and transpiration both in *Commelina communis*

and in tomato (Wilkinson and Davies, 1997; Wilkinson et al., 1998; Jia and Davies, 2007). As changes in pH define the dissociation state of weak acids, among them the major phytohormones abscisic acid (ABA) and indol acetic acid (IAA, auxin), they would thereby affect both their distribution between the apoplast and the cellular compartments of the plant, and hence, their biological activities. This has been shown, for example, for ABA accumulation in the alkalinizing xylem sap of a gradually dehydrated detached cotton leaf, which could be prevented by a pretreatment with an H^+-ATPase-activating fungal toxin, fusicoccin (Hartung et al., 1988).

Moreover, xylem sap pH is likely a crucial component of the proton-motive force governing transmembrane transport between the xylem and the surrounding BSCs. Yet, in spite of its importance to the plant basic life processes, molecular evidence linking a specific H^+-ATPase to the pH regulation of the leaf xylem sap and to the ensuing physiological changes in the leaf is missing.

H^+-ATPases constitute a family of proton pumps driven by hydrolysis of ATP and are found exclusively in the plasma membrane of plants and fungi (Axelsen and Palmgren, 2001). 11 H^+-ATPases isoforms have been reported in Arabidopsis; among them, the AHA1 and AHA2 are by far the most abundantly expressed members of this family throughout plant life and tissues (Haruta et al., 2010). The expression of GUS reporter gene in Arabidopsis, under the *AHA2* promoter, revealed abundant expression specifically in roots and leaves, and especially in the vascular tissue (Fuglsang et al., 2007). Our transcriptome analysis of protoplasts isolated from Arabidopsis BSCs and mesophyll cells (MCs) showed that the BSCs express the *AHA2* gene at a threefold higher level than the MCs, while the *AHA1* gene expression, though abundant, was not different between these two cell types (Wigoda et al., 2017). Here we show (a) that it is mainly the activity of AHA2 which acidifies the sap, and (b) that the xylem sap pH regulates the radial hydraulic conductance of the leaf.

Materials and Methods

Plant material

Plant types. We used WT (wild type) *Arabidopsis thaliana* plants ecotype Colombia, Col-0 (aka Col) and T-DNA insertion *AHA* mutants (Col), obtained from SALK institute (http://signal.salk.edu/cgi-bin/tdnaexpress), *AHA1* mutants: *aha1-6* (SALK_ 016325), *aha1-7* (SALK_ 065288) and *aha1-8* (SALK_ 118350), and *AHA2* mutants; *aha2-4* (SALK_ 082786)

and *aha2-5* (SALK_022010) obtained from the Arabidopsis Biological Resource Center (Ohio State University). The plants genotypes were determined by PCR with allele-specific primers and then the single-gene knockout were confirmed using real time PCR (RT-PCR) for the absence of *AHA2* RNA. The sequences of the PCR primers are provided in the supplemental Table S1.

Plant Growth Conditions. All plants were grown in soil as described by (Shatil-Cohen et al., 2011). Plants were kept in a growth chamber under short-day conditions (10-h light) and a controlled temperature of 20–22°C, with 70% humidity and constant fluorescent lights (Osram cool white, T5 FH 35W/840 HE, Germany), light intensity at the plant level of 100-150 µmol m^{-2} sec^{-1}. The plants were irrigated twice a week.

Leaf perfusion. Leaves from 6-7 week old plants, approximately 2.5 cm long and 1 cm wide, were excised at the petiole base using a sharp blade and immediately dipped in "xylem perfusion solution" (XPS, see Solutions below), in 0.5 ml Eppendorf tubes for 30 minutes. Perfusion experiments using Safranin O (Sigma cat. #: S2255; 1% w/v in XPS) demonstrated that 30 minutes incubation sufficed for the whole leaf perfusion via the petiole by means of the transpiration stream (Fig. S1)

Determination of xylem sap pH in detached leaves

The leaf xylem pH was determined using the dual-excitation membrane-impermeant fluorescent dye fluorescein isothiocyanate conjugated to 10 kD dextran (FITC-D; (Hoffmann and Kosegarten, 1995; Mühling et al., 1995). An *in-vivo* pH calibration curve was constructed using XPS buffered to predefined pH values (5, 5.5,6, 6.5, 7 and 7.5; see Solutions below). Effects of vanadate in high-K^+ solution or of fusicoccin in low-K^+ solution (i.e., in XPS) was tested in the absence of pH buffers (see Solutions below).

Sample preparation on the microscope stage. Immediately after the leaf xylem perfusion, the leaf was washed with that leaf's intended perfusate (the specific XPS to be tested) without the dye, laid on a microscope slide adaxial side up, and a drop of this XPS (without the dye) was placed on top. Then, a thin layer of silicone high vacuum grease (Merck cat. #: 1.07921.0100) was applied around the leaf edge and a large coverslip (50 by 20 mm, larger than the leaf) was placed on the leaf and affixed to the slide beneath. The minor veins on the adaxial side were imaged via the coverslip.

Fluorescence microscopy was *p*erformed using an inverted microscope (Olympus-IX8 integrated within the Cell-R system, http://www.olympus-global.com), via an UPlanSApo 10*X*/0.40(∞ /0.17/ FN26.5) objective. Pairs of images were recorded at two excitation wavelengths of 488

nm and 450 nm, and a single emission wavelength of 520 nm (Hoffmann and Kosegarten, 1995; Mühling et al., 1995), with a 12-bit CCD camera, Orca-AG (Hamamatsu, http://www.hamamatsu.com).

In all fluorescence microscopy experiments, each treatment was performed on at least five leaves, each from a different plant, on three days (all together, five biological repetitions per treatment, three independent experiments), alternating randomly among different treatments. Four to six paired images of a minor vein were obtained from different areas of each leaf (four-six technical repetitions per a biological repeat). For background values, leaves were perfused with experimental solutions without the dye; one such leaf was sampled per treatment or plant type on each day of an experiment (all together, at least three biological repetitions per treatment or plant type, a total of 20 leaves, with three technical repetitions per each biological repeat).

Image analysis. The acquired pairs of images were exported in linear 16-bit tiff format for further processing with ImageJ (ver. 1.49V; http://rsbweb.nih.gov/ij/). The pixel by pixel ratio of the two images in each pair was calculated using the ImageJ 'Ratio-plus' plugin (Paulo J. Magalhães, 2004). The ratio calculation took into account the average background fluorescence at the corresponding excitation wavelength, which was subtracted from each pixel's fluorescence. Further analysis was performed on selected pixels, based on the image resulting from excitation at 488 nm. Only pixels with fluorescence values below the camera saturation level (<4095) and, at the same time, of at least 3 times the mean background value were selected (areas enclosed within yellow lines in the supplemental Fig. S2C). For each leaf (biological repeat), the mean fluorescence ratio obtained from a vein segment was converted to a pH value, using an *in-vivo* calibration curve, which was obtained, as described above, from paired images of WT leaves fed with pH calibration solutions (see Solutions below). We occasionally verified the system stability using an *in-vitro* calibration curve, derived from imaging drops of the calibration solutions placed on microscope slides rather than fed into leaf veins. Also, changing the composition of the buffers (MES and HEPES) in the XPS had no effect on the calibration curve.

Physiological characterization of the leaf (gas exchange and hydraulic conductance, K_{leaf})

Sample preparation. For Fig. 4 (and Suppl Fig. S5), the leaves were excised in the dark, shortly after "lights OFF" transition, their petioles were dipped in the unbufferred High-K^+ XPS and placed in gas-sealed transparent 25 cm x 25 cm X15 plastic boxes with water-soaked tissue paper on the bottom in order to provide ~100% humidity, for the duration of the night. Measurements were conducted in the morning, between 10:00 AM to 12:00 PM, after 20 min

illumination in the growth chamber. For Fig. 5 (and Suppl. Fig. S6), leaves were excised in the dark just before "lights ON" transition and their petioles were dipped in vials with buffered XPS* (at pH, 6 and 7.5; see Solutions below). The vials were placed in gas-sealed transparent plastic boxes as described above. The boxes were then kept for two hours in the growth room under the regular light and temperature conditions. Prior to the measurements, the boxes were opened for 3 minutes to equilibrate with the ambient vapor pressure deficit (VPD) of 1.3-1.5 kPa. The measurements were conducted between 10:00AM and 1:00 PM (3-5 hours after lights ON).

Gas-exchange assays, i.e., g_s (stomata conductance) and E (transpiration) were performed (as in (Sade et al., 2014) using a Li-Cor 6400 portable gas-exchange system (LI-COR, USA https://www.licor.com/) equipped with a standard leaf cuvette with an aperture of 2 x 3 cm^2). The transfer time from box to Licor was at most 5 s. The measuring conditions were set to be as similar as possible to the growth chamber conditions (illumination: 150 µmol m^{-2} s^{-1}; the amount of blue light was set to 10% of the photosynthetically active photon flux density to optimize stomatal aperture, the leaf temperature: approximately 24 °C, the VPD: approximately 1.3 kPa, and [CO_2] surrounding the leaf: 400 µmol mol^{-1}).

Measuring the leaf water potential, Ψ_{leaf}. Immediately following the gas exchange measurements, the leaf was transferred to a pressure chamber (ARIMAD-3000; MRC Israel) equipped with a home-made silicon adaptor especially designed to fit Arabidopsis petioles into the chamber's O-ring. Ψ_{leaf} was determined as described in (Sade et al., 2014).

K_{leaf} ; Determination of the leaf hydraulic conductance. K_{leaf} was calculated for each individual leaf (Martre et al., 2000) by dividing the whole-leaf's E (transpiration, i.e., the water flux rate) by $\Delta\Psi_{Leaf}$ (the pressure gradient along the water path from the dipped leaf petiole to outside of stomata, which we replaced here by Ψ_{Leaf} , i.e., leaf water potential, since the petiole was dipped in XPS at a nearly null water potential).

Solutions

FITC-D dye (Sigma cat. #: FD10S) was added from a 10 mM stock in water (kept aliquoted, protected from light, at -20 ^oC) to all the XPS (except in the autofluorescence assays) to a final conc. of 100 µM.

XPS, Xylem Perfusion Solution: 1 mM KCl, 0.3 mM $CaCl_2$ and 20 mM D-sorbitol (Sigma cat# 8143). Upon preparation, when unbuffered, the pH of this solution was 5.6 -5.8 and its osmolarity was approx. 23 mOsm/L.

Low-K^+ XPS: the same as XPS above.

High-K^+ XPS: XPS + 10 mM KNO_3 and D-sorbitol adjustment to the same osmolarity as the low-K^+ XPS. Upon preparation, the pH of this solution was 5.6 -5.8.

XPS*: High-K^+ XPS buffered with 10 mM MES and 10 mM HEPES and buffered to pH 6 or 7.5 with NMG. These solutions were adjusted with D-sorbitol to a final osmolarity of 40 mOsm/L.

pH calibration solutions: XPS buffered with 20 mM MES and HCl or N-Methyl D-glucamine (NMG) to pH 5, 5.5, or 6), or with 20 mM HEPES and NMG to pH 6.5, 7, or 7.5. Osmolarity of these solutions was adjusted with D-sorbitol to 23 mOsm/L.

Solutions for leaf physiological characterization: Non-buffered High-K^+ XPS (as above) was used for Figure 4 (and Suppl. Fig. S5). XPS* was used for Fig. 5 (and Suppl. Figs. S6).

Generation of SCR:AHA2-complemented plants

Vector construction: *AHA2* gene was cloned into pDONR™ 221 (Invitrogene) vector and the SCR promoter into pDONRP4P1r using Gateway® compatible by BP reactions, and later cloned into the pB7M24GW (Invitrogene) two fragment binary vector by LR reaction according to the manufacturer's instructions. The binary *SCR:AHA2* vector was transformed into Agrobacterium by electroporation; transformants were selected on LB plates containing 25 µg/ml gentamycin and 50 µg/ml spectinomycin.

aha2-4 and aha2-5 mutant lines transformation with *SCR:AHA2* was performed using the floral dip method (Clough and Bent, 1998). Transformants were selected based on their BASTA resistance, grown on plates with MS (Murashige and Skoog, Duchefa cat# M222.0050) Basal medium + 1 % sucrose and 20 µg/ml BASTA (Glufosinate Ammonium, Sigma cat # 45520). DNA insertion was verified in selected lines by PCR targeting the junction of *AHA2* and the 35S terminator with forward primer about 1000bp from the 3' end of AHA2 and reverse primer on the 35S terminator (see primer list in supplemental Table S1).

AHA2 Gene Expression in the whole leaf by qRT-PCR

RNA extraction and quantitative real-time (qRT-) PCR. Total RNA was extracted from leaves using Tri-Reagent (Molecular Research Center, cat. #: TR 118) and treated with RNase-free DNase (Thermo Scientific™, cat. #: EN0525). Complementary DNA (cDNA) was prepared using the EZ-First Strand cDNA synthesis kit (Biological Industries cat. #: 2080050) according to the manufacturer's instructions. qRT-PCR was performed using C1000 Thermal Cycler (Bio-Rad), in the presence of EvaGreen (BIO-RAD cat.# 172-5204) and PCR primers to amplify specific regions of the genome (*16*; supplemental Table S1). The results were analyzed using Bio Rad CFX manager™ software. Dissociation curve analysis was performed at the end of each qRT-PCR reaction to validate the presence of a single reaction product and lack of primer

dimerization. Expression levels of examined genes were normalized using two normalizing genes (AT5G12240 and AT2G07734, *18*)

Statistics

The Student's t-test was used for comparison of two means, which were considered to be significantly different at $P < 0.05$. For comparisons of three or more population means we used ANOVA, all-pairs Tuckey HSD (JMP® Pro 13), wherein different letters represent statistical differences at $P<0.05$. Images which yielded extreme ratio values which were more than 2 SD above the mean were discarded.

Results

We used the fluorescence of FITC-dextran (10 kD) perfused via petioles into detached WT Arabidopsis leaves to monitor the pH within the leaf minor veins (Supplementary Materials and methods, Supplementary Figs S1-S3). We first stimulated the vascular H^+-pumps by feeding the xylem with fusicoccin (a fungal stimulator of P-type proton pumps, *20*). Indeed, a sharp decrease in xylem sap pH of about two pH units compared with leaves in control conditions (Figs. 1Ai, 1Aii, 1B) was measured approximately 30 minutes after addition of 10 µM fusicoccin. ETOH, the fusicoccin solvent, by itself, had no impact on xylem pH (Suppl. Fig. S3).

Further, WT leaves treated with 1 mM of vanadate (a commonly used P-type H^+-pump inhibitor (reviewed by *21*), in a high-K^+ solution (i.e., in the presence of added 10 mM KNO_3), resulted in xylem sap alkalization of about one pH unit within 30-40 min (Figs. 1Aiii, 1Aiv, 1C). Interestingly, neither a similar exposure to vanadate in the low-K^+ solution (XPS without added KNO_3, supplemental Fig.S4A), nor the high-K^+ solution by itself (Suppl. Fig. S4B) had any effect on the xylem sap pH.

In an attempt to resolve between the relative contributions of the two abundant H^+-ATPAses of the BSCs, AHA1 and AHA2, to the acidification of the xylem pH, we compared the xylem sap pH of WT plants to T-DNA insertion mutants of either pump. We used two independent mutant lines with a homozygous loss of function of the *AHA2* gene (*aha2-4* and *aha2-5*) and three such lines with mutated *AHA1* gene (*aha1-6, aha1-7, aha1-8*; Suppl. Materials and methods). The xylem sap pH of both *AHA2* mutants, *aha2-4* and *aha2-5*, was consistently higher, by 0.5-1 pH units, compared to the WT plants (Fig. 2A). However, among the three lines of *AHA1* mutants, only in one line, *aha1-8*, was the xylem sap pH higher by about 1 pH unit compared to WT and in the other two lines, *aha1-6* and *aha1-7*, the xylem sap pH was not significantly different from WT (Fig. 2B).

To test further the ability of AHA2 to acidify the xylem sap pH, we complimented the *AHA2* deficient plants (the *aha2-4* mutant), with the *AHA2* gene directed specifically to the BSCs (under the BSCs-specific promotor Scarecrow SCR, *22*). Using qRT-PCR on whole leaves of mature transgenic plants, we confirmed *AHA2* absence in the *aha2-4* mutant (Fig. 3A, as in *16*), and demonstrated successful complementation in two lines (T55 and T56). The transcript level of *AHA2* gene in these lines was even higher than in the WT (Fig. 3A). While the xylem sap pH in the *AHA2*-knockout mutant, *aha2-4*, was more alkaline than in WT plants (repeating the results of Fig. 2A above), upon the complementation of the *aha2-4* mutant with the BSC-directed *AHA2*, the xylem sap pH in both lines became no different from WT (Fig 3B). The level of *AHA1* transcript in the whole leaf was not affected by the genetic manipulations of AHA2, neither by *AHA2* mutation (as in *17*), nor by the BSC-specific mutant complementation with *AHA2* (Fig. 3C).

To examine the impact AHA2 on the water economy of the whole leaf we determined the leaf water potential (Ψ_{leaf}) and its transpiration (E), and from these two calculated the leaf hydraulic conductance (K_{leaf}). We compared the hydraulic conductance (K_{leaf}) in detached leaves of WT and the *aha2-4* and *aha2-5* knockouts fed with unbuffered XPS. Notably, the K_{leaf} of the mutants was appreciably lower than that of WT leaves, about 50 % in *aha2-4* and only about 30 % in *aha2-5* (Fig. 4 and Suppl. Fig. S5). Furthermore, WT leaves perfused with XPS buffered at pH 7.5 had K_{leaf} lower by over 50% compared to WT leaves perfused with XPS buffered at pH 6 (Fig. 5 and Suppl. Fig. S6).

Discussion

H^+-ATPases are well known regulators of the apoplastic pH, which has a key role in the cell ion homeostasis (Taiz and Zeiger, 2014). Here we demonstrate, for the first time, that AHA2, residing in the BSCs plasma membrane, exerts a dominant role in the regulation of the xylem sap pH in leaves. This conclusion is based on four different complementing approaches used in our study.

(1) *In vivo, direct and accurate measurement of xylem pH*. The ratio of fluorescence intensity of FITC-dextran excited at two different wavelengths is independent of the absolute dye concentration and is related only to pH. By this dual excitation technique, any variations in dye concentration caused by dye loading, compartmentation, leakage and photo-bleaching can be compensated for, since these parameters have a similar effect on fluorescence intensities at both

wavelengths. Having introduced this technique, Hoffmann (Hoffmann et al., 1992) and Hoffmann and Kosegarten (Hoffmann and Kosegarten, 1995) successfully measured the apoplastic pH, pH gradient between various cell types in the apoplast of sunflower leaves, and changes of leaf apoplastic pH in response to the uptake of NH_4^+ and NO_3^- via petioles. In maize, measurements using pH-sensitive microelectrodes validated FITC-dextran as a faithful reporter of apoplastic pH-conditions (Pitann et al., 2009). In using the membrane-impermeable FITC-dextran fed to the Arabidopsis leaf via a petiole, we relied on earlier demonstrations of the tight isolation of the vascular system due to the bundle sheath (Kinsman and Pyke, 1998; Shatil-Cohen et al., 2011; Shatil-Cohen and Moshelion, 2012; Sade et al., 2014; Wigoda et al., 2017). We were thus satisfied that the FITC probe remained confined and reported reliably on the pH from within the BSCs-lined xylem apoplast of the minor veins (Fig. 1A).

(2) *The use of classical pharmacological agents*, an H^+-ATPases specific enhancer (fusicoccin) and inhibitor (vanadate), fed directly to the leaf xylem, established that pH acidification of the leaf xylem sap involves P-type proton pump(s) (AHAs), which extrude protons – most likely, from the BSCs – into the xylem lumen. Notably, in our experiments, vanadate increased the xylem sap pH only when it was administered in high-K^+ XPS, while vanadate in low-K^+ XPS, did not cause any detectable pH change. We explain this requirement for 10 mM KNO_3 to show vanadate inhibition of H^+-pump, as resulting from increased concentration of substrate (the added K^+ and NO_3^- ions) which can participate in secondary H^+-co-transport into the BSCs, thereby dissipating the protons from the xylem lumen. This conforms with the aforementioned general notion that the pH of an apoplastic compartment reflects, among others, a balance in the bi-directional proton movements (Serrano, 1988). That proton-coupled K^+ transmembrane co-transport plays a particularly important role in the BSCs, is suggested by the 10% higher expression in BSCs (relative to mesophyll cells) of two K^+ uptake permeases, AtKT2 and AtKUP11 (likely to be H^+-coupled; (Wigoda et al., 2017) and references therein).

(3) *Genetic manipulation – -knockouts.* We have established here, for the first time, the dominant role of AHA2 in regulating the xylem sap pH in Arabidopsis leaf, by contrasting the consistently lower pH determined in the xylem sap of WT and the consistently higher pH in AHA2 mutant lines, a*ha2-4* and *aha2-5*, while the *aha1* mutants did not exhibit consistently higher xylem sap pH. This phenotype has not yet been described.

(4) *Genetic manipulation – knockout complementation.* Moreover, the xylem sap pH was restored to WT-like levels in two lines resulting from *aha2-4* complementation with an *AHA2*

gene directed specifically into the BSCs, using the specific promotor SCR. Surprisingly, although the complementation was directed to BSCs, the AHA2 transcript levels in the whole leaf of the complemented plants were considerably higher than in the WT leaf. The lack of a change of the transcript of AHA1, not only in the mutant aha2-4, as already noted by (Haruta et al., 2010), but also in the complementation lines T55 and T56 (Fig. 3C) is another indication for the already inferred specificity of AHA2 for the maintenance of xylem sap pH. Nevertheless, the level of AHA2 activity – as reflected in the xylem sap pH (especially in the complemented line T55, where pH was intermediate between the mutant *aha2-4* and the WT) – was somewhat less than could be expected from the transcript level. This suggest a strong post-transcriptional regulation of the AHA2 in BSCs.

AHA2 role in the regulation of the whole leaf water balance. The notion that AHA pumps, in general, power secondary H^+-cotransport across cell membranes facing the apoplast is decades old – (reviewed, for example, by *19*, *20*, *26*, *27*)). The plant plasma membrane H^+-ATPase has been since recognized as essential for plant growth (reviewed by (Falhof et al., 2016)). The practically sole "celebrated product" of its action to date is the proton motive force (PMF) – a gradient of protons without or in combination with an electrical gradient – which drives the movement of solutes across cellular membranes. Notwithstanding, only in a few cases has the plasma membrane H^+-ATPase been assigned a *specific* physiological role – mainly in stomatal physiology and in roots (reviewed by (Falhof et al., 2016)). Here we show for the first time another, novel aspect of transport activity regulated by AHA2 – that of water fluxes from the xylem into the leaf and across the bundle sheath layer – evident as the leaf hydraulic conductance, K_{leaf}. We demonstrate here an inverse, causative correlation between the resulting K_{leaf} and the xylem sap pH, be it pH manipulated directly by buffers, or altered by genetically by abolishing AHA2 activity (in *AHA2* knockouts).

The results of this study broaden our basic understanding of how a leaf controls its water influx. In an earlier work, Shatil-Cohen et al.,(Shatil-Cohen et al., 2011) localized K_{leaf} to the BSCs layer by showing that K_{leaf} decreased when the BSCs were brought into direct contact with the plant stress hormone, abscisic acid (ABA) fed to the detached leaf, and not when ABA was smeared on the leaf surface. We may hypothesize here, that it was the xylem sap pH – elevated perhaps due to ABA inhibition of AHA2 (similar to the inhibition seen in guard cells) – that mediated also the above ABA effect on the K_{leaf}.

Moreover, we now propose that K_{leaf} decline caused by abiotic stress, is mediated by xylem sap alkalinization caused by the abiotic stress. Furthermore, we suggest that xylem sap alkalinization mediates also the decline in nutrient uptake due to abiotic stress. AHA2, which we found instrumental in generating the low pH in the leaf xylem sap, builds up the PMF which powers the secondary, proton-coupled export and import of solutes across the BSCs membranes and into the leaf thus regulating plant nutrition. Xylem sap alkalinization means a decline in the PMF. Since PMF very likely drives also the extrusion of toxic compounds from the xylem-lining cells into the xylem, the xylem sap pH (i.e., activity of AHA2 of the BSCs, its primary regulator) should govern also the plant toxicity tolerance. These hypotheses await future experimentation.

In conclusion, rapid growth rate and high yields of crop plants are positively correlated with enhanced transpiration and K_{leaf}. Our finding that AHA2 regulates K_{leaf} via xylem sap pH provides a molecular basis for understanding a novel aspect, other than just PMF, of the control that the leaf xylem sap pH can exert. This control, in combination with effects of PMF, is bound to underlie the plant's key physiological activities. These results provide a new focus for exploration and understanding the role of the involvement of BSCs in determining the xylem sap composition. BSCs are likely to become a key target tissue for the development of a new generation of manipulations for plant adaptation to environmental challenges.

Acknowledgments

We thank Ms. Dvorah Weisman for help with image analysis. This research was supported by the Israel Science Foundations, ISF (grants No.1312/12, and 1842/13 to NM, grant No. 878/16 to MM and a grant No. 12-01-0007 from the Israeli Chief Scientist, Ministry of Agriculture & Rural Development to MM and NM).

Competing interests

All authors declare they have no competing interests.

Supplementary Materials

Figure S1. Perfusion of detached leaves via petioles

Figure S2. Image analysis details

Figure S3. Fusicoccin (FCC) itself and not its solvent EtOH lowered the leaf xylem sap pH

Figure S4. Neither vanadate in the *low-K*$^+$ XPS nor the high-K$^+$ XPS *without* vanadate affect the xylem sap pH in WT Arabidopsis

Figure S5. Knockout of AHA2 or alkaline xylem sap pH decrease K_{leaf} in detached leaves

Figure S6. Alkaline xylem sap pH decreases K_{leaf} in detached WT leaves.

Table S1. List of primers used for genotyping (PCR) and expression quantification (RT-PCR) of AHA1 and AHA2 in mutants and transformed plants.

References and Notes

Axelsen KB, Palmgren MG (2001) Inventory of the superfamily of P-type ion pumps in Arabidopsis. Plant physiology **126**: 696–706

Clough SJ, Bent AF (1998) Floral dip: A simplified method for Agrobacterium-mediated transformation of Arabidopsis thaliana. Plant Journal **16**: 735–743

Falhof J, Pedersen JT, Fuglsang AT, Palmgren M (2016) Plasma Membrane H+-ATPase Regulation in the Center of Plant Physiology. Molecular Plant **9**: 323–337

Fuglsang AT, Guo Y, Cuin T a, Qiu Q, Song C, Kristiansen K a, Bych K, Schulz A, Shabala S, Schumaker KS, et al (2007) Arabidopsis protein kinase PKS5 inhibits the plasma membrane H+ -ATPase by preventing interaction with 14-3-3 protein. The Plant cell **19**: 1617–34

Grignon C, Sentenac H (1991) pH and ionic conditions in the apoplast. Annual Review of Plant Physiology and Plant Molecular Biology **42**: 104–121

Hartung W, Radin JW, Hendrix DL (1988) Abscisic Acid Movement into the Apoplastic solution of Water-Stressed Cotton Leaves: Role of Apoplastic pH. Plant physiology **86**: 908–913

Haruta M, Burch HL, Nelson RB, Barrett-Wilt G, Kline KG, Mohsin SB, Young JC, Otegui MS, Sussman MR (2010) Molecular characterization of mutant Arabidopsis plants with reduced plasma membrane proton pump activity. The Journal of biological chemistry **285**: 17918–29

Hoffmann B, Kosegarten H (1995) FITC-dextran for measuring apoplast pH and apoplastic pH gradients between various cell types in sunflower leaves. Physiologia Plantarum **95**: 327–335

Hoffmann B, Planker R, Mengel K (1992) Measurements of pH in the apoplast of sunflower leaves by means of fluorescence. Physiologia Plantarum **84**: 146–153

Jia W, Davies WJ (2007) Modification of leaf apoplastic pH in relation to stomatal sensitivity to root-sourced abscisic acid signals. Plant physiology **143**: 68–77

Kinsman EA, Pyke KA (1998) Bundle sheath cells and cell-specific plastid development in Arabidopsis leaves. Development (Cambridge, England) **125**: 1815–1822

Lamdan NL, Attia Z, Moran N, Moshelion M (2012) The Arabidopsis-related halophyte Thellungiella halophila: boron tolerance via boron complexation with metabolites? Plant, cell & environment **35**: 735–46

Marre E (1979) Fusicoccin: A Tool in Plant Physiology. Annual Review of Plant Physiology **30**: 273–288

Martre P, Durand JL, Cochard H (2000) Changes in axial hydraulic conductivity along elongating leaf blades in relation to xylem maturation in tall fescue. New Phytologist **146**: 235–247

Mengel K (1994) Iron availability in plant tissues-iron chlorosis on calcareous soils. Plant and Soil **165**: 275–283

Mühling KH, Plieth C, Hansen U, Sattelmacher B (1995) Apoplastic pH of intact leaves of Vicia faba as influenced by light. Journal of Experimental Botany **46**: 377–382

Palmgren MG (2001) Plant plasma membrane H+ATPases: Powerhouses for nutrient uptake.

Pantin F, Monnet F, Jannaud D, Costa JM, Renaud J, Muller B, Simonneau T, Genty B (2013) The dual effect of abscisic acid on stomata. New Phytologist **197**: 65–72

Paulo J. Magalhães (2004) Ratio Plus (ImageJ).

Pitann B, Kranz T, Mühling KH (2009) The apoplastic pH and its significance in adaptation to salinity in maize (Zea mays L.): Comparison of fluorescence microscopy and pH-sensitive microelectrodes. Plant Science **176**: 497–504

Sade N, Shatil-Cohen A, Attia Z, Maurel C, Boursiac Y, Kelly G, Granot D, Yaaran A, Lerner S, Moshelion M (2014) The role of plasma membrane aquaporins in regulating the bundle sheath-mesophyll continuum and leaf hydraulics. Plant physiology **166**: 1609–20

Serrano R (1988) Structure and function of proton translocafing ATPase in plasma membranes of plants and fungi. Biochimica et Biophysica Acta (BBA) - Reviews on Biomembranes **947**: 1–28

Shapira O, Israeli Y, Shani U, Schwartz A (2013) Salt stress aggravates boron toxicity symptoms in banana leaves by impairing guttation. Plant, Cell and Environment **36**: 275–287

Shapira O, Khadka S, Israeli Y, Shani U, Schwartz A (2009) Functional anatomy controls ion distribution in banana leaves: Significance of Na + seclusion at the leaf margins. Plant, Cell and Environment **32**: 476–485

Shatil-Cohen A, Attia Z, Moshelion M (2011) Bundle-sheath cell regulation of xylem-mesophyll water transport via aquaporins under drought stress: a target of xylem-borne ABA? The Plant journal : for cell and molecular biology **67**: 72–80

Shatil-Cohen A, Moshelion M (2012) Smart pipes: the bundle sheath role as xylem-mesophyll barrier. Plant signaling & behavior **7**: 1088–91

Sze H, Li X, Palmgren M (1999) Energization of plant cell membranes by H+-pumping ATPases. Regulation and biosynthesis. The Plant cell **11**: 677–690

Taiz L, Zeiger E (2014) Plant Physiology and Development. doi: 10.3119/0035-4902-117.971.397

Wigoda N, Pasmanik-Chor M, Yang T, Yu L, Moshelion M, Moran N (2017) Differential gene expression and transport functionality in the bundle sheath versus mesophyll – a potential role in leaf mineral homeostasis. Journal of Experimental Botany **68**: 3179–3190

Wilkinson S, Corlett JE, Oger L, Davies WJ (1998) Effects of Xylem pH on Transpiration from Wild-Type and flacca Tomato Leaves1. Plant physiology **117**: 703–709

Wilkinson S, Davies WJ (1997) Xylem Sap pH Increase: A Drought Signal Received at the Apoplastic Face of the Guard Cell That Involves the Suppression of Saturable Abscisic Acid Uptake by the Epidermal Symplast. Plant physiology **113**: 559–573

Wysocka-Diller JW, Helariutta Y, Fukaki H, Malamy JE, Benfey PN (2000) Molecular analysis of SCARECROW function reveals a radial patterning mechanism common to root and shoot. Development (Cambridge, England) **127**: 595–603

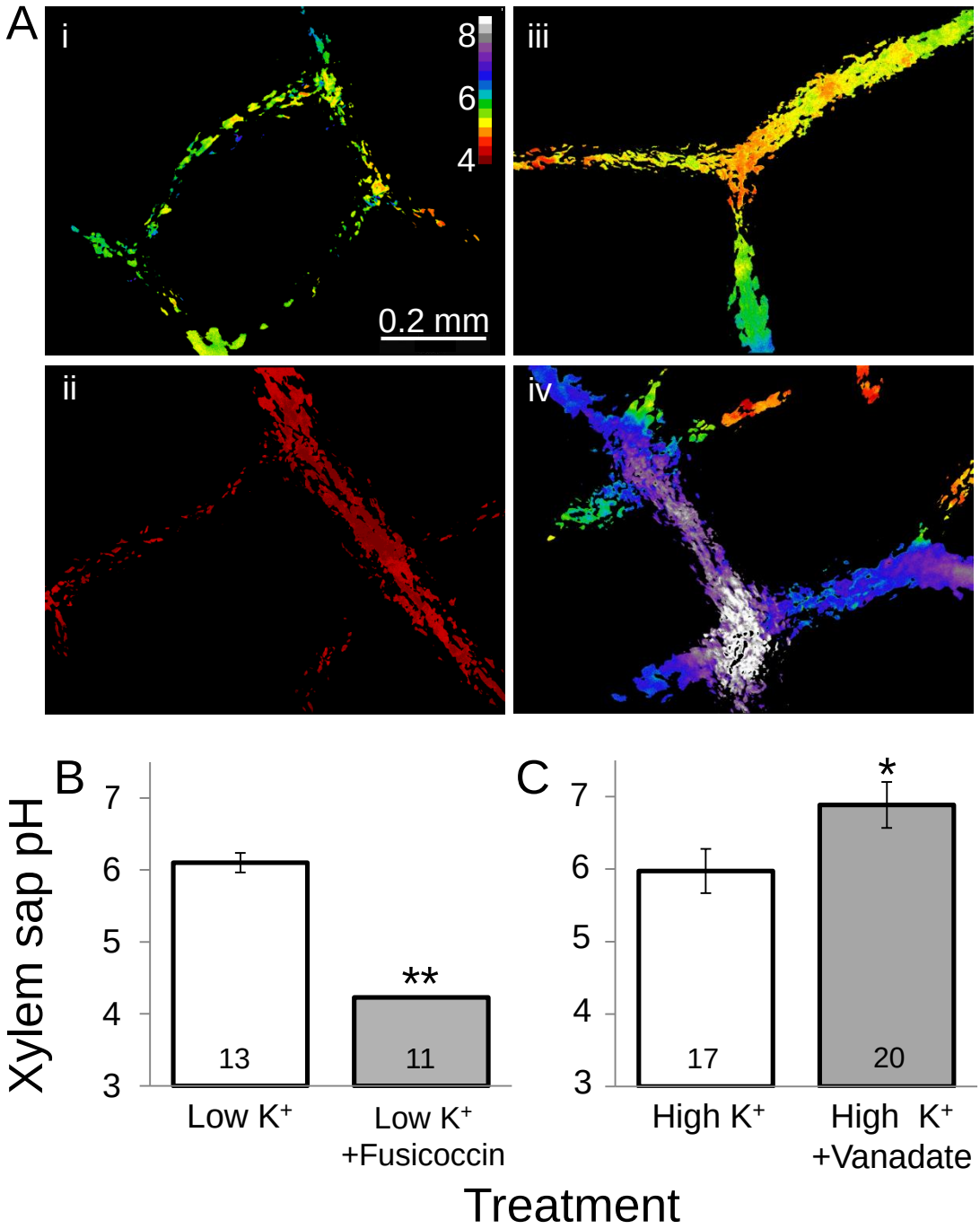

FIGURE 1. Leaf xylem sap pH reduced by petiole-fed fusicoccin (an AHA stimulator), and increased by vanadate (an AHA inhibitor) in minor veins in detached leaves of WT (wild type) Arabidopsis. **A.** Representative images of treatment effects with color-coded pH values calculated ratiometrically for all pixels which passed the selection criteria (Supplementary Materials and methods), with black masking all other pixels. i, low-K^+ control (i.e., XPS, xylem perfusion solution). ii, XPS + fusicoccin (10 μM). iii, high-K^+ control solution (XPS +10 mM KNO_3). iv, XPS +10 mM KNO_3 + vanadate (1 mM Na_3VO_4). **B.** The mean (±SE) xylem sap pH without and with fusicoccin in the indicated number of leaves (biological repeats) from at least three independent experiments. Asterisks denote significant differences from the respective control, using Student's two-tailed unpaired t-test (*: $P < 0.05$, **: $P < 0.001$). Where error bar is invisible, SE= 0.009. Other details as in A. **C.** The mean (±SE) calculated values of the xylem sap pH without and with vanadate. Other details as in B.

Fig. 1. Wigoda, Grunwald et al, 2017

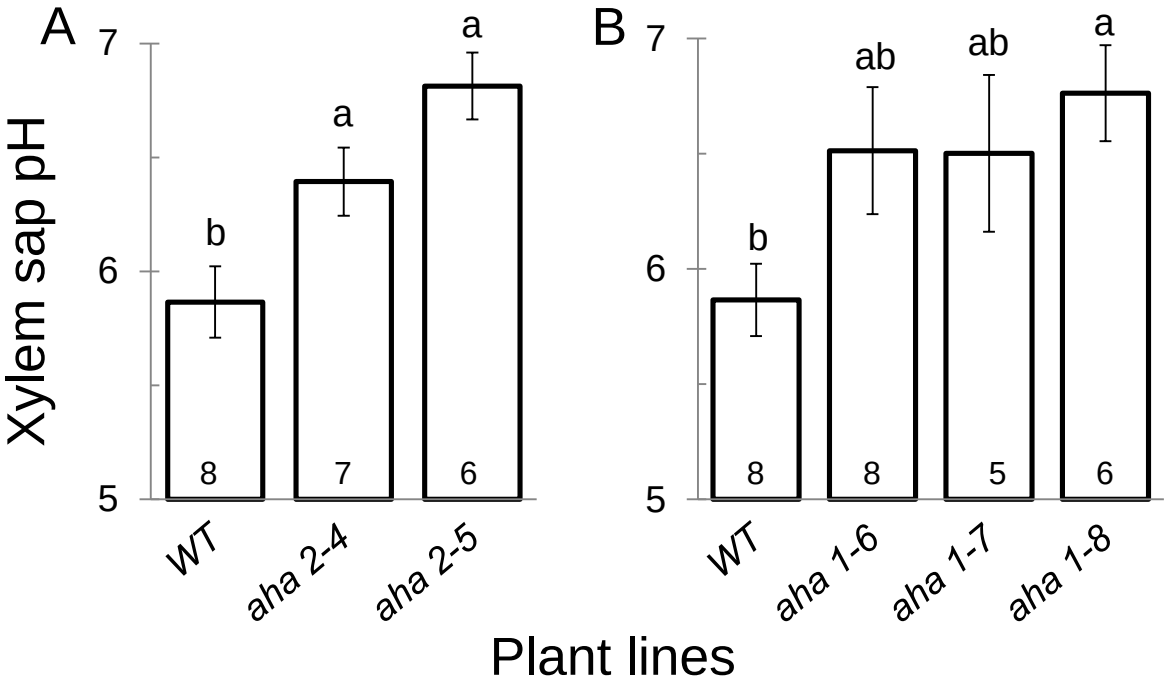

FIGURE 2. Knockout of *AHA2* increases xylem sap pH in minor leaf veins of Arabidopsis leaf. A. *aha2* knockout lines and WT plants. The mean (±SE) xylem sap pH in the indicated number of leaves, from three independent experiments. Different letters denote significantly different pH values (P< 0.05; ANOVA). **B.** *aha1* knockout lines and WT plants. Other details as in A.

Fig. 2. Wigoda, Grunwald et al, 2017

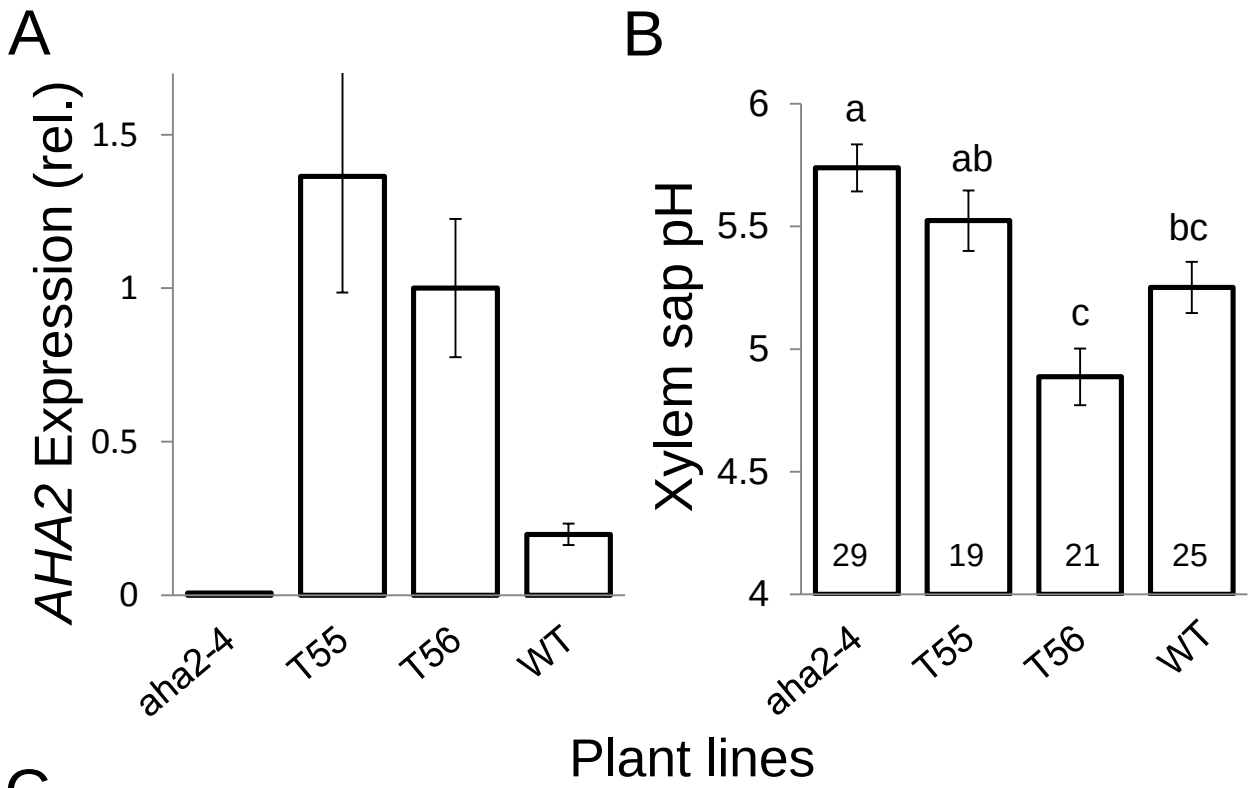

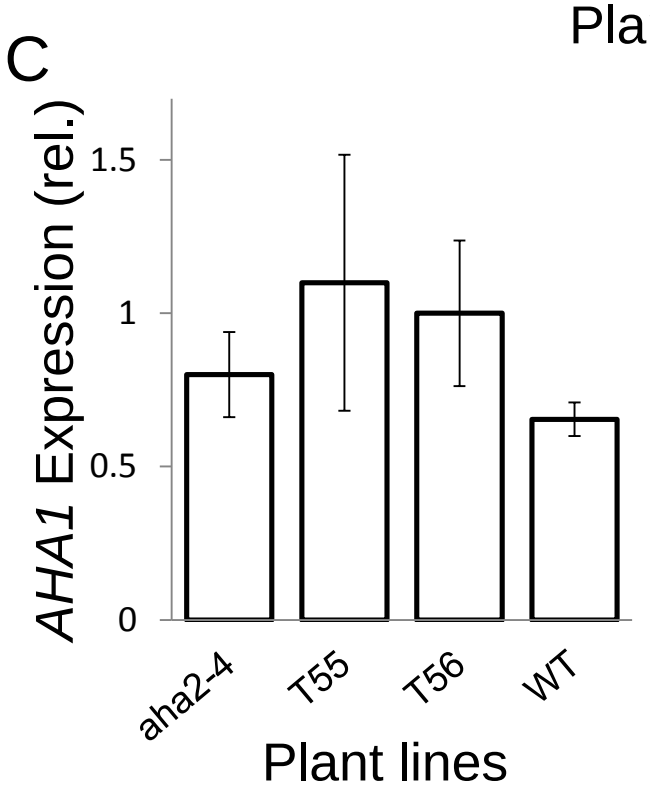

FIGURE 3. Expression levels of *AHA2* and *AHA1* and xylem sap pH in leaves of WT, *aha2-4*, and in two independent bundle-sheath-specific AHA2-complimented lines (T55, T56). **A.** Mean normalized (±SE) *AHA2* expression levels obtained by qRT-PCR on whole leaf RNA (n=5 biological repetitions, leaves; see Suppl. Materials and methods). **B.** Mean (±SE) xylem sap pH in the indicated number of leaves from three independent experiments. Different letters indicate significantly different means (P<.0.05; ANOVA). **C.** Mean normalized (±SE) *AHA1* expression levels; other details as in A.

Fig. 3. Wigoda, Grunwald et al, 2017

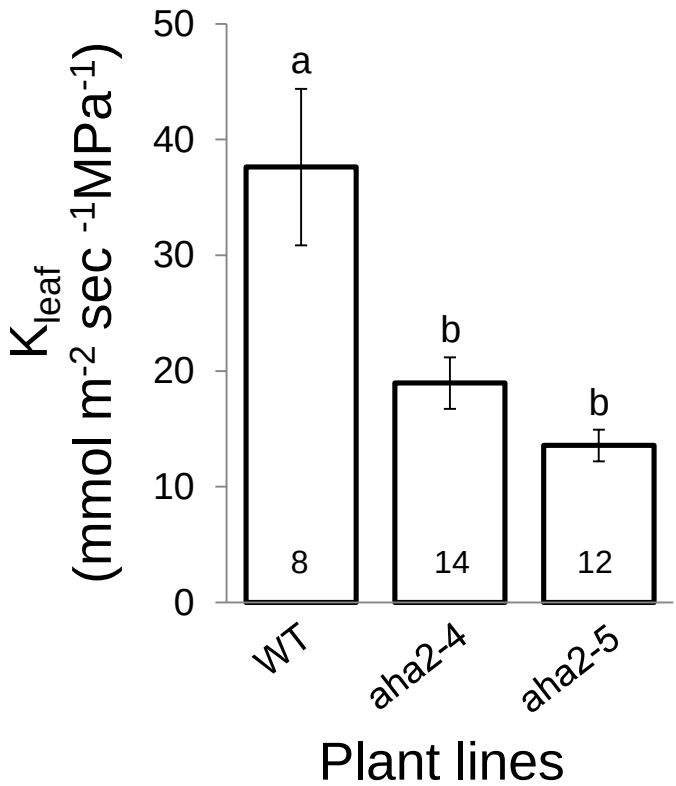

FIGURE 4. The leaf hydraulic conductance (K_{leaf}) depends on the activity of AHA2. Mean (±SE) K_{leaf} (calculated as in Suppl. Fig. S5A) in detached leaves of WT Arabidopsis and of *AHA2* knockouts perfused with non-buffered XPS. Numbers are those of assayed leaves. Different letters indicate significantly different means (P<.0.05; ANOVA). Note that K_{leaf} is lower in the *AHA2* knockouts relative to WT.

Fig. 4. Wigoda, Grunwald et al, 2017

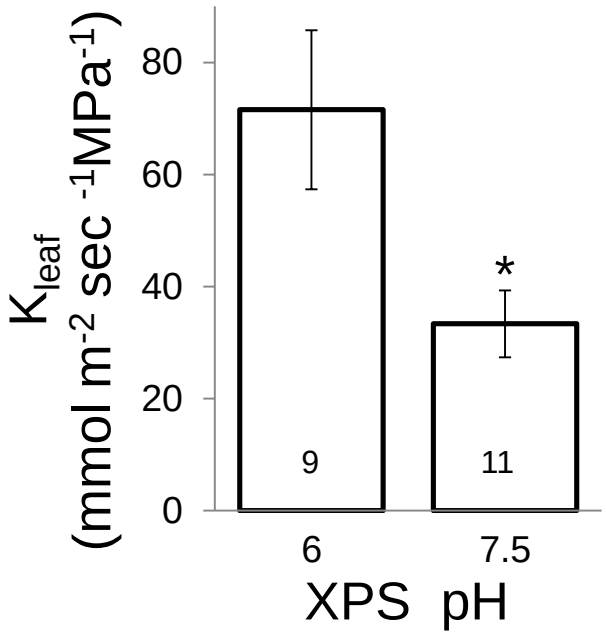

FIGURE 5. The leaf hydraulic conductance (K_{leaf}) regulated by the pH of the xylem perfusion solution (XPS). Mean (±SE) K_{leaf} (calculated as in Suppl.Fig. S5B) of the indicated numbers of detached leaves of WT Arabidopsis fed with XPS pH-buffered as indicated, from three independent experiments. Different letters indicate significantly different means (P<.0.05; Students t-test). Note that K_{leaf} is lower at alkaline pH relative to acidic pH.

Fig. 5. Wigoda, Grunwald et al, 2017